Game-Theoretic Spectrum Trading in RF Relay-Assisted Free-Space Optical Communications

Game-Theoretic Spectrum Trading in RF Relay-Assisted Free-Space Optical Communications

Shenjie Huang, *Member, IEEE*, Vahid Shah-Mansouri, *Member, IEEE*, and Majid Safari, *Member, IEEE*

***Abstract*—Free-space optical (FSO) communication offers wireless connectivity with high data rates and low system complexity; however, it suffers from the infrequent adverse weather conditions. This work proposes a novel hybrid RF/FSO system based on a game theoretic spectrum trading process to enhance the reliability of FSO links. The proposed system is considered to be both spectrum- and power-efficient. It is assumed that no RF spectrum is preallocated to the FSO link and only when the link availability is severely impaired by the infrequent adverse weather conditions, i.e. fog, etc., the source can borrow a portion of licensed RF spectrum from one of the surrounding RF nodes. A market-equilibrium-based pricing process is proposed for the spectrum trading between the source and RF nodes. By using the leased spectrum, the source is able to establish a dual-hop RF/FSO hybrid link to maintain its throughout to the destination. Our extensive performance analysis illustrates the effectiveness of the proposed communication system. It is demonstrated that the proposed scheme can significantly improve the average capacity of the system, especially when the surrounding RF nodes are with low traffic loads. In addition, the system benefits from involving more RF nodes into the spectrum trading process by means of diversity. Finally, the application of the proposed system in a realistic scenario is presented based on the weather statistics in the city of Edinburgh, UK, which demonstrates that the system can substantially enhance the link availability towards the carrier-class requirement.**

I. Introduction

In recent decades, the scarcity in the radio frequency (RF) spectrum becomes the bottleneck in the expansion of wireless communication networks. As a potential candidate for the long-range wireless connectivity, free-space optical (FSO) communication has attracted widespread and significant interest in both scientific community and industry because of its high achievable data rates, license-free spectrum, outstanding security level and low installation cost. FSO has numerous applications and in particular it is considered as a cost-effective wireless backhaul solution of the future 5G systems [1]. However, there exist some limitations and challenges in practical FSO systems including the pointing and misalignment loss due to building sways [2] and unpredictable connectivity in the presence of atmosphere due to the turbulence-induced intensity fluctuation (also known as scintillation) and adverse weather conditions such as rain, snow and fog [3].

Numerous techniques have been proposed to effectively mitigate the effects of beam misalignment fading (e.g., employing beamwidth optimization [4] and adaptive tracking systems [5]) and scintillation (e.g., using spatial diversity [6] and multi-hop relaying [7]). Unlike the spatially dynamic channel fluctuations caused by misalignment and scintillation, the attenuations due to adverse weather conditions are fairly static both in time and space, which makes the above solutions ineffective [8]. Studies have shown that the adverse weather conditions can significantly deteriorate FSO link by introducing an optical power attenuation of up to several hundreds of decibels per kilometer [9]. A possible strategy to effectively improve the FSO link availability against adverse weather conditions is the so-called *hybrid RF/FSO* [10]. The motivation behind this idea is that because of the distinct carrier frequencies, FSO links are more susceptible to scattering due to fog and turbulence-induced scintillation whereas RF links are more sensitive to rain conditions (especially for frequencies above 10 GHz). Therefore, with the help of additional RF link, the hybrid RF/FSO systems can enjoy higher availability than a traditional FSO link.

In the literature, there are basically two main types of hybrid RF/FSO systems based on either switch-over or simultaneous transmission. In switch-over transmission (also called hard-switching transmission) scheme, the RF link is simply a backup link and data is transmitted through either of the channels. In [11], a low-complexity hard-switching hybrid RF/FSO system with both single-threshold and dual-threshold for FSO link operation is proposed. Besides the theoretical studies, several experimental works focusing on this type of hybrid link have also been reported [12]. Although switch-over hybrid RF/FSO link is simple and has also been employed in some commercial FSO products [3], the preallocation of RF spectrum to a backup link with occasional use is inherently spectrum-inefficient [13].

In another type of hybrid RF/FSO links, simultaneous data transmission is considered where both the FSO and RF links are simultaneously active. One simple implementation of such hybrid links is sending the same data on both channels concurrently and decoding the signal at the receiver based on the more reliable channel [14] or the maximal ratio combining of two channels [15]. Some other works focus on the designs of joint channel coding and decoding over the two channels in the hybrid link. In particular, the hybrid rateless coding is employed so that the coding rate for each channel in the hybrid link can be adapted to the data rate that the channel can provide and no channel knowledge at the transmitter is required [16]. Furthermore, the hybrid RF/FSO systems are also modelled as two independent parallel channels to further improve the total throughout [17], [18]. Although hybrid RF/FSO links with simultaneous transmission outperform those with switch-

S. Huang and M. Safari are with the School of Engineering, the University of Edinburgh, Edinburgh (e-mail: {shenjie.huang, majid.safari}@ed.ac.uk). V. Shah-Mansouri is with the School of Electrical and Computer Engineering, University of Tehran, Tehran (e-mail: vmansouri@ut.ac.ir).

over transmission, they require both FSO and RF link to be active continuously even when the FSO link is in good conditions and itself is able to support the required data throughput. Therefore, in the absence of power allocation strategy, hybrid RF/FSO links with simultaneous transmission are power-inefficient and may also generate unneeded RF interference to the environment [11], [15].

Game theory has been widely employed in the context of cognitive radio networks for resource management. For instance, in [19] a power allocation strategy for a two-tier femtocell network with a central macrocell underlaid with multiple femtocells is investigated using the Stackelberg game. Besides the application in power allocation, game theory is also employed in solving spectrum allocation issues. Particularly, in [20] three different game theory based pricing models including market-equilibrium, competitive and cooperative pricing models are proposed to solve the spectrum allocation between licensed and unlicensed users in a cognitive radio network. However, the application of game theory in the hybrid RF/FSO systems has not been well investigated.

In this work, in order to aid FSO technology to achieve high availability against adverse weather conditions, we propose a novel hybrid RF/FSO system based on the game theoretic spectrum trading. We assume that there exists a preinstalled FSO link between the source and destination; however, no RF spectrum is preallocated to this link. When the link availability is significantly impaired by the infrequent long-term adverse weather conditions, the source attempts to borrow a portion of RF spectrum from one of the surrounding RF nodes, which have licensed spectrum to communicate with the destination, to establish a dual-hop RF/FSO hybrid link[1] and maintain its throughput to the destination. A market-equilibrium-based pricing process is proposed for the spectrum trading between the source and RF nodes. At the source, the spectrum demand is defined as a function of the unit spectrum price by maximizing the source's utility. At each RF node, the spectrum supply function is also calculated by maximizing its own utility. The market-equilibrium price is then achieved by calculating the cross point of the spectrum demand and supply functions [20]. Compared to above-mentioned hybrid RF/FSO systems in the literature, the proposed system is considered to be spectrum-efficient since no preallocation of RF spectrum to the link is necessary and the source borrows the RF spectrum only when it is needed. In addition, the investigated system is considered to be power-efficient since the hybrid link is only established during the infrequent adverse weather conditions. Furthermore, the proposed system is also cost-effective by borrowing RF spectrum from surrounding RF nodes rather than establishing and always maintaining a high-cost RF link[2]. To the best of authors' knowledge, this is the first time the game-theoretic spectrum trading is employed to design a hybrid RF/FSO system with high availability. The effectiveness of the proposed architecture in the improvement of both average capacity and availability is also confirmed through the numerical results.

[1]Note that different from the traditional hard-switching hybrid RF/FSO links in the literature where data is transmitted through either the FSO link or RF link [11], [16], in the proposed system the FSO link turns to a hybrid link rather than a pure RF relay link in adverse weather conditions. Although in adverse weather conditions the capacity of FSO link can be significantly reduced, keeping it active even with a relatively low data rate would still improve the overall throughput compared to the system with a pure RF link.

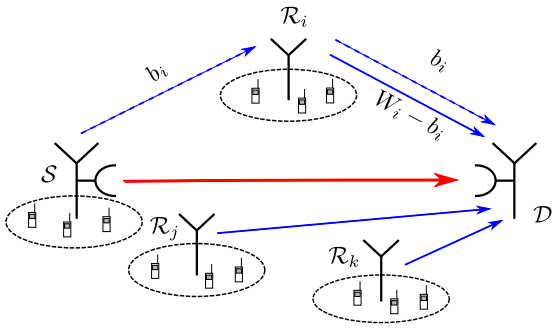

Fig. 1. The proposed system model in practical application for wireless backhauling. $\mathcal{S}$: the source; $\mathcal{R}$: the surrounding RF nodes; $\mathcal{D}$: the destination; b_i: the leased bandwidth; W_i: the total licensed bandwidth the ith RF node is allocated for backhauling.

The rest of this paper is organized as follows. The channel model and system description are shown in Section II. Section III presents the derivations of demand and supply functions and describes the spectrum trading scheme and relay selection strategy in detail. The numerical results and discussion are presented in Section IV. Finally, we conclude this paper in Section V.

II. System Model

Fig. 1 shows the schematic of the proposed system for the application of wireless backhauling in a heterogeneous network consists of a large macro-cell and numerous small cells. The source $\mathcal{S}$ denotes the small cell base station (SBS) which requires high data throughput to the macro-cell base station (MBS), i.e., the destination $\mathcal{D}$ and the RF nodes $\mathcal{R}_i$ with $i \in \{1, \ldots, N\}$ are the surrounding SBSs that have wireless backhaul connectivity to $\mathcal{D}$ using licensed sub-6 GHz spectrum W_i. The source $\mathcal{S}$ would like to send its information to the destination $\mathcal{D}$ and there exists an already installed FSO link between them. When the data rate of FSO link goes below a specific rate, the source broadcasts a request signal to the surrounding N distributed RF nodes for the sake of buying a portion of their spectrum and establishing a hybrid dual-hop RF/FSO link to improve its data rate to the MBS. Compared to the line-of-sight (LoS) RF backhauling with unlicensed high-frequency spectrum (e.g., millimeter-wave), the RF backhauling with low-frequency licensed spectrum is also widely investigated [16]–[18] due to its advantage of non-LoS property and lower installation cost, which makes it more attractive on small-cell networks especially in urban areas [1], [21]. The proposed novel communication scheme can also be employed in other applications where the surrounding RF

[2]This could be any type of RF link: if sub-6 GHz RF link is used the cost of licensing is high; whereas if high-frequency line-of-sight RF link is used the link itself is costly [1]).

nodes are any types of relay nodes in LTE-based wireless backhaul architecture.

A. Channel Model

Since both FSO and RF links are involved in the proposed system, the channel models for both channels need to be investigated.

1) ***FSO link****:* Considering that adaptive tracking systems are employed to properly address the misalignment fading, the FSO link $\mathcal{S}-\mathcal{D}$ suffers from two main channel impairments including the turbulence-induced scintillation and adverse weather condition whereas at very different time scales. The scintillation is a short-term effect with coherence time T_s on the order of several milliseconds [5]; however, the weather condition is a long-term effect with time-scale T_c on the order of hours [16]. Assuming that the FSO link employs the intensity modulation direct detection (IM/DD), the received electrical signal expression can be written as

$$s_o = \rho g_o h_o x_o + z_o, \tag{1}$$

where ρ is the the responsivity of the photodetector, g_o refers to the average gain to the receiver optical power, h_o denotes the random turbulence-induced intensity fading, x_o is the transmitted optical intensity, s_o is the received electrical signal and z_o is zero-mean real Gaussian noise with variance σ_o^2. Note that we use the subscript 'o' to denote the optical link. The signal-independent Gaussian noise z_o in (1) arises from thermal noise as well as the shot noise induced by the ambient light. The average gain g_o can be expressed as [17], [22]

$$g_o = \left[\mathrm{erf}\left(\frac{\sqrt{\pi}d}{2\sqrt{2}\phi L_{SD}}\right)\right]^2 \times e^{-\kappa L_{SD}}, \tag{2}$$

where the first and second terms denote the geometric loss due to the divergence of the transmitted beam and weather-related atmospheric loss due to scattering and absorption, respectively, d is the receiver aperture diameter, ϕ is the beam divergence angle, L_{SD} is the distance between the source and the destination, and κ is a weather-dependent attenuation coefficient determined based on the Beer-Lambert law. The relationship between κ and the visibility V in km can be expressed as [9]

$$\kappa = \frac{3.91}{V}\left(\frac{\lambda_o}{550\times 10^{-9}}\right)^{-\zeta}, \tag{3}$$

where λ_o is optical wavelength and ζ is the size distribution of the scattering particles equal to 1.6, 1.3 and $0.585V^{1/3}$ when $V>50$, $6\le V\le 50$ and $V<6$, respectively.

There are several ways to model the turbulence-induced intensity fluctuation h_o such as log-normal distribution and Gamma-Gamma distribution. In this work, we employ the Gamma-Gamma distribution which can describe the intensity function within a wide range of turbulence conditions as [22]

$$f_{h_o}(x) = \frac{2\left(\alpha\beta\right)^{(\alpha+\beta)/2}}{\Gamma(\alpha)\Gamma(\beta)} x^{(\alpha+\beta)/2-1} K_{\alpha-\beta}\left(2\sqrt{\alpha\beta x}\right), \tag{4}$$

where $\Gamma(\cdot)$ is the Gamma function, $K_p(\cdot)$ is the modified Bessel function of the second kind. The parameter α and β are given by

$$\alpha = \left[\exp\left(\frac{0.49\chi^2}{\left(1+0.18\vartheta^2+0.56\chi^{12/5}\right)^{7/6}}\right)-1\right]^{-1},$$
$$\beta = \left[\exp\left(\frac{0.51\chi^2\left(1+0.69\chi^{12/5}\right)^{-5/6}}{\left(1+0.9\vartheta^2+0.62\vartheta^2\chi^{12/5}\right)^{5/6}}\right)-1\right]^{-1}, \tag{5}$$

respectively, where $\chi^2 = 0.5C_n^2 k^{7/6} L_{SD}^{11/6}$, $\vartheta^2 = kd^2/4L_{SD}$ and $k = 2\pi/\lambda_o$. Note that C_n^2 is the turbulence refraction structure parameter. For IM/DD FSO channel given in (1), the achievable rate (channel capacity lower bound) in the presence of average transmitted optical power constraint, i.e., $E[x_o]\le P_o$, conditioned on the random channel gain h_o can be expressed as [23, Eq.(26)]

$$C_o = \frac{W_o}{2}\log_2\left(1+\frac{e\rho^2 g_o^2 h_o^2 P_o^2}{2\pi\sigma_o^2}\right), \tag{6}$$

where e refers to the natural logarithm base and W_o is the bandwidth of the FSO link. Note that different from the traditional AWGN channel capacity expression in RF, the SNR term in (6) is proportional to the squared optical power due to the employed intensity modulation.

In the proposed system, setting a reasonable performance metric to decide whether the FSO link is satisfactory or not is crucial, since the FSO link status would trigger the switch between FSO-only link and hybrid RF/FSO link. To smooth out the quick FSO link capacity fluctuations introduced by scintillation, we employ the sliding window averaging strategy introduced in [24]. Note that a window with relatively longer interval than the scintillation coherence time T_s should be considered so that the measured average FSO link capacity can accurately reflect the current long-term weather condition. The measured average FSO link capacity over the window interval is selected as the performance metric which is approximated as $\overline{C}_o = E\left[C_o\right]$ where $E[\cdot]$ denotes the ensemble expectation. The source keeps monitoring the FSO link condition and calculating $\overline{C}_o$ every window interval. When $\overline{C}_o$ is lower than the trigger rate C_{th}, the spectrum trading process is triggered to establish the dual-hop RF relay link, whereas when it exceeds C_{th}, the source stops buying the RF spectrum. To ensure that the source could make a quick response to the change of weather conditions, the window interval should be set much less than the time-scale of the weather changes T_c. Also note that C_{th} can be any positive values and larger C_{th} indicates the spectrum trading game is easier to be triggered, which results in more frequent spectrum trading events and also higher system complexity.

2) ***RF link****:* In this work, it is assumed that the source does not establish and maintain a direct RF link along the FSO link to the destination, but instead it uses the borrowed spectrum from surrounding RF nodes to relay its data to the destination only when needed. When a RF node $\mathcal{R}_i$ is selected by the source as the relay to realize the dual-hop $\mathcal{S}-\mathcal{R}_i-\mathcal{D}$ link, this RF relay channel can be expressed as

$$s_{R,i}^{(t)} = \sqrt{g_{R,i}^{(t)}} h_{R,i}^{(t)} x_{R,i}^{(t)} + z_{R,i}^{(t)}, \tag{7}$$

where the subscript 'R' is used to denote the RF link, $t = 1, 2$ refer to the RF link from the source to the relay ($\mathcal{S} - \mathcal{R}_i$ link) and that from the relay to the destination ($\mathcal{R}_i - \mathcal{D}$ link), respectively, $s_{R,i}^{(t)}$ and $x_{R,i}^{(t)}$ are the received and transmitted signal, respectively, $g_{R,i}^{(t)}$ denotes the average power gain, $h_{R,i}^{(t)}$ is the RF fading coefficient and $z_{R,i}^{(t)}$ refers to the zero-mean complex Gaussian noise with power spectrum density N_0. By expressing the RF relay channel as (7), it is assumed that the relay operates in the half-duplex mode. It means that the relay can either receive from the source or transmit to the destination over the RF link and cannot do both simultaneously [17], [18]. As a result, there is no interference between two sub-links. For RF signal transmission it is considered that Gaussian codebooks are employed at transmitters, which means at every symbol duration the transmitted symbol $x_{R,i}^{(t)}$ is generated independently based on a zero-mean rotationally invariant complex Gaussian distribution [17]. The total RF transmitted power, i.e., $E[|x_{R,i}^{(t)}|^2]$, at the source and the relay are denoted as $P_R^{\mathcal{S}}$ and $P_R^{\mathcal{R}}$, respectively. The average power gain $g_{R,i}^{(t)}$ can be expressed as [17]

$$g_{R,i}^{(t)} = \left[\frac{\sqrt{G_{TX}G_{RX}}\lambda_R}{4\pi L_{\rm ref}}\right]^2 \times \left(\frac{L_{\rm ref}}{L_{R,i}^{(t)}}\right)^{\delta}, \tag{8}$$

where G_{TX} and G_{RX} refer to the RF transmitter and receiver gain, respectively, λ_R denotes the RF wavelength, $L_{\rm ref}$ is the reference distance for the antenna far-field, $L_{R,i}^{(t)}$ denotes the link distance with $t = 1, 2$ for $\mathcal{S} - \mathcal{R}_i$ and $\mathcal{R}_i - \mathcal{D}$ link, respectively, and δ refers to the RF path-loss exponent. Note that the average power gain $g_{R,i}^{(t)}$ is associated with the specific distance between the source (relay) and relay (destination) and the fading coefficient $h_{R,i}^{(t)}$ can be described by distinct models such as Rayleigh, Rician or Nakagami-m fading in different application scenarios [1], [15], [25].

According to the channel expression of RF links given in (7), the channel capacity of the $\mathcal{S} - \mathcal{R}_i$ link and $\mathcal{R}_i - \mathcal{D}$ link for source's data transmission can be expressed as

$$\begin{aligned} C_{R,i}^{(1)}(b_i) &= b_i \log_2\left(1 + \frac{g_{R,i}^{(1)}|h_{R,i}^{(1)}|^2 P_R^{\mathcal{S}}}{N_0 b_i}\right), \\ C_{R,i}^{(2)}(b_i) &= b_i \log_2\left(1 + \frac{g_{R,i}^{(2)}|h_{R,i}^{(2)}|^2 P_R'}{N_0 b_i}\right), \end{aligned} \tag{9}$$

respectively, where b_i is the size of spectrum borrowed from the relay, W_i is the total licensed spectrum that the ith relay possesses for $\mathcal{R}_i - \mathcal{D}$ link and P_R' is the power allocated by the RF node for transmitting the source's data to the destination. Note that in (9) the spectral efficiency of $\mathcal{S} - \mathcal{R}_i$ link is related to the size of the leased spectrum b_i. This is because the transmitted RF power is assumed to be fixed, hence increasing b_i would introduce more noise and reduce the received SNR which results in the decrease of the spectral efficiency [26]. On the other hand, by assuming that the RF node allocates the total transmitted power for source's data transmission proportional to b_i, i.e., $P_R' = P_R^{\mathcal{R}} b_i / W_i$, the SNR of $\mathcal{R}_i - \mathcal{D}$ link can be expressed as $g_{R,i}^{(2)}|h_{R,i}^{(2)}|^2 P_R^{\mathcal{R}} / N_0 W_i$. Therefore, the spectral efficiency of $\mathcal{R}_i - \mathcal{D}$ link is not associated with b_i. With the expressions of the RF link capacity given in (9), the capacity of the decode-and-forward RF link $\mathcal{S} - \mathcal{R}_i - \mathcal{D}$ can be written as [21]

$$C_{R,i}(b_i) = \min\left\{q_i\, C_{R,i}^{(1)}(b_i)\,, (1 - q_i)\, C_{R,i}^{(2)}(b_i)\right\}, \tag{10}$$

where $q_i \in (0, 1)$ refers to a time sharing variable. We use q_i to indicate the fraction of time when $\mathcal{S} - \mathcal{R}_i$ link is active and hence $1 - q_i$ denotes the time fraction when $\mathcal{R}_i - \mathcal{D}$ link is active[3]. Note that the capacity of the RF relay link can be expressed as in (10) on the condition that the RF relay is operated on a half-duplex mode [17], [18].

Lemma 1. *Denote the spectral efficiencies of $\mathcal{S} - \mathcal{R}_i$ link and $\mathcal{R}_i - \mathcal{D}$ link as*

$$\eta_{\rm sr}(b_i) = \log_2\left(1 + \frac{r_i}{b_i}\right) \text{ and } \eta_{{\rm rd},i} = \log_2\left(1 + \frac{g_{R,i}^{(2)}|h_{R,i}^{(2)}|^2 P_R^{\mathcal{R}}}{N_0 W_i}\right), \tag{11}$$

respectively, with $r_i = g_{R,i}^{(1)}|h_{R,i}^{(1)}|^2 P_R^{\mathcal{S}} / N_0$. By choosing the optimal time sharing variable, the maximal capacity of the dual-hop $\mathcal{S} - \mathcal{R}_i - \mathcal{D}$ link can be expressed as

$$C_{R,i}(b_i) = \frac{b_i\, \eta_{{\rm rd},i}\, \eta_{\rm sr}(b_i)}{\eta_{\rm sr}(b_i) + \eta_{{\rm rd},i}}. \tag{12}$$

Proof. Since the first term in the min function of (10) is a monotonically increasing function of q_i and the second term is a monotonically decreasing function of q_i, for a given shared spectrum b_i the optimal q_i^* to maximize $C_{R,i}$ is given by the cross point of the two functions as

$$q_i^* = \frac{\eta_{{\rm rd},i}}{\eta_{\rm sr}(b_i) + \eta_{{\rm rd},i}}. \tag{13}$$

This optimal time sharing variable (13) indicates that the capacities of $\mathcal{S} - \mathcal{R}_i$ and $\mathcal{R}_i - \mathcal{D}$ links are identical, which means all the data transmitted to the relay can be successfully transferred to the destination. By substituting (13) into (10) one can hence get the maximal capacity of the dual-hop $\mathcal{S} - \mathcal{R}_i - \mathcal{D}$ link as given in (12).

In order to check the monotonicity of $C_{R,i}(b_i)$, one can take the first derivative of it as

$$\begin{aligned} \mathcal{T}(b_i) &= \frac{{\rm d}C_{R,i}(b_i)}{{\rm d}b_i} \\ &= \frac{\eta_{{\rm rd},i}\left[\eta_{\rm sr}(b_i)\right]^2 + \eta_{{\rm rd},i}^2 \eta_{\rm sr}(b_i) - \frac{\eta_{{\rm rd},i}^2}{\ln 2}\left[1 - 2^{-\eta_{\rm sr}(b_i)}\right]}{\left[\eta_{\rm sr}(b_i) + \eta_{{\rm rd},i}\right]^2}. \end{aligned} \tag{14}$$

It can be proved that $\mathcal{T}(b_i) > 0$ holds for all $b_i \geq 0$ and approaches to zero for $b_i \to +\infty$, thus $C_{R,i}(b_i)$ is a monotonically increasing function of b_i with a saturated value $r_i/\ln 2$ at high b_i. ■

B. Spectrum Trading Game

We consider that each RF node has data traffic and hence has its own backhaul data to transmit to the destination using a maximum allocated bandwidth W_i via the $\mathcal{R}_i - \mathcal{D}$ link.

[3]It is worth noting that the RF node continuously transmits its own backhaul data using the remaining $W_i - b_i$ spectrum.

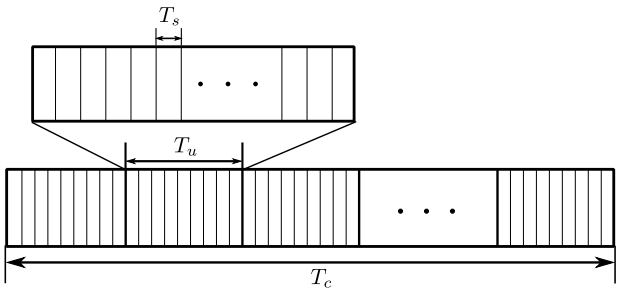

Fig. 2. Time scales: T_s, the coherence time of the scintillation; T_c, the coherence time of the weather condition; T_u, time duration of using the leased RF spectrum before repeating the game.

Particularly, in wireless backhaul application presented in Fig. 1 this data traffic comes from the connected user equipments (UEs) in the small cell. In addition, it is assumed that different RF nodes are allocated non-overlapping frequency spectrum for data transmission so that there is no interference between them at the destination [27]. When RF nodes are not in high traffic load, they might be willing to lend part of their spectrum to the source and obtain some revenues at the expense of self-data transmission limitation. In the wireless backhaul application, this limitation may affect the QoS performance of the connected UEs in the small cells.

When the RF nodes notice that the source requests to buy their spectrum due to its non-functional FSO link condition, a two-player game is operated between the source and each RF node. In this paper, we consider a market-equilibrium-based pricing approach for the spectrum trading game [20], [28], [29] where the source is treated as the *buyer* and the RF relay nodes are treated as the *sellers*. It is assumed that different RF nodes are not aware of each other[4] and each seller has to negotiate with the source and sets their price independently to meet the buyer's demand according to their own utilities. In the spectrum trading game (discussed later in Section III), both source and RF nodes in the system are considered to be rational and selfish so that they only focus on their own payoff and always follow the best strategies which maximize their own utility. When all games (or negotiations) between source and RF nodes are finished, the source receives the distinct unit spectrum prices proposed by different RF nodes and the sizes of spectrum that they want to lend. Based on this received information, the source is able to decide on the best RF node. By notifying the selected RF node, a dual-hop RF relay link $\mathcal{S}-\mathcal{R}_i-\mathcal{D}$ can be established and the previous FSO link $\mathcal{S}-\mathcal{D}$ turns to a hybrid dual-hop RF/FSO link. The proposed system with single RF relay selection benefits from its simplicity. However, it is also possible for the source to borrow RF spectrum from multiple RF nodes simultaneously rather than routing its traffic from a single node (similar to the system investigated in [31] in the context of RF relaying system), which can be an interesting work to address in the future.

[4]In practice, this assumption is justified due to the lack of any centralized controller or information exchange among RF nodes. When the RF nodes have more information about each other, more complicated spectrum trading games can be investigated such as competitive and cooperative games [20], [30].

The result of the spectrum trading game mainly depends on the condition of the RF relay link and the traffic load supported by surrounding RF nodes. As a result, the source should repeat the relay selection when these conditions significantly change. Denote the coherence time of the fading in RF link and traffic loads in surrounding nodes as T_f and T_t, respectively. For wireless RF links with fixed transceivers, the temporal behaviour of the fading is more stable compared to the mobile channels and is tightly related to the existence of LoS and environmental conditions (e.g., the vehicular traffic). It is concluded that T_f in the fixed wireless RF links is typically on the order of seconds [25], [32]. On the other hand, T_t is relatively longer which depends on different application scenarios and could vary from several seconds to hours. Therefore, it is reasonable to assume that the source uses the leased RF spectrum for a time period of $T_u = \min\{T_f, T_t\}$ before involving into a new spectrum trading game and possibly updating the selected RF relay. The time scales considered in this work are plotted in Fig. 2. Invoking the discussion of the coherence time of scintillation T_s and weather change T_c in Section II-A, one can get that T_u is much shorter than T_c but much longer than T_s. Therefore, in every T_c interval the source should repeat the RF relay selection based on the updated information every T_u interval.

III. Solution of Spectrum Trading

In this section, we present the solution of the game-theoretic spectrum trading process for the proposed communication setup. Note that similar to the traditional hard-switching based hybrid RF/FSO systems investigated in the literature [11], the switch here should be triggered under specific conditions. As mentioned before, we consider that it is triggered when the FSO link capacity is below a trigger rate, i.e., $\overline{C}_o < C_{th}$. We employ a market-equilibrium-based pricing model in which, for a given unit spectrum price, the *buyer* (source) chooses its spectrum demand based on its *demand function* and the *sellers* (the surrounding RF nodes) set the amount of spectrum they would like to offer according to their *supply function*. The demand function indicates the willingness of the source to buy the spectrum, whereas the supply function idicates the willingness of the RF nodes to sell the spectrum. The market-equilibrium refers to the price in which the spectrum demand of the source equals to the spectrum supply of the relays and no excess supply exists in the market [28], [29]. In the proposed system, the same spectrum trading process (game) should be applied between the source and each surrounding RF node. Without loss of generality, we firstly focus on the spectrum trading between the source $\mathcal{S}$ and the RF nodes $\mathcal{R}_i$ and derive the spectrum demand and supply functions individually. Later, the calculation of the market-equilibrium price using the supply and demand functions is discussed and the relay selection strategy is presented.

A. Utility of Source and the Demand Function

To quantify the spectrum demand of the source when $\mathcal{R}_i$ is selected as the relay node, the utility gained by the source

can be expressed as a non-linear equation

$$\mathcal{U}_i = B - \omega \left\{ \left(R_N - \left[\overline{C}_o + C_{R,i}(b_i) \right] \right)^+ \right\}^2 - b_i p_i, \quad (15)$$

where $x^+ = \max(x, 0)$, B refers to the revenue obtained from serving its local users, ω denotes the constant weight for the cost of QoS degradation, R_N is the nominal rate of the FSO link in clear weather, b_i is the borrowed spectrum, $p_i \in (0, +\infty)$ is the unit spectrum price offered by the RF node $\mathcal{R}_i$, and $\overline{C}_o$ and $C_{R,i}(b_i)$ denote the current FSO link capacity and RF relay link capacity, respectively. In (15), the second term denotes the cost introduced by the QoS degradation of the service it provides and the third term refers to the cost of buying spectrum from RF node. The practical meaning behind the utility given in (15) is the obtained benefit through spectrum borrowing minus the corresponding costs. Note that FSO link is usually employed to offer high data rate, therefore the nominal rate R_N is a quite large value on the order of several Gbps [3]. In adverse weather condition, the FSO link capacity is significantly reduced, hence even with the help of RF relay link, the nominal rate (or the data rate requirement) is hard to be achieved, hence the utility (15) can then be rewritten as

$$\mathcal{U}_i = B - \omega \left\{ R_N - \left[\overline{C}_o + C_{R,i}(b_i) \right] \right\}^2 - b_i p_i. \quad (16)$$

The coefficient ω shown in (16) measures the desirability of the source to the extra data rate provided by the RF link. Higher ω indicates higher cost of QoS degradation and therefore the source are more motivated to borrow the spectrum by paying higher price. If the source borrows more spectrum from the RF node, although higher throughput can be achieved and hence less QoS degradation of the local users, it also results in higher cost. Therefore, for a given spectrum price the optimal borrowed spectrum which maximizes the utility can be determined. The so-called demand function refers to the spectrum demand that maximizes the utility function (16) when the spectrum price p_i is given [28]. To achieve the demand function, substituting (12) into (16) the optimization problem at $\mathcal{S}$ can be expressed as follows:

$$\max_{b_i} \ \mathcal{U}_i = B - \omega \left\{ R_N - \left[\overline{C}_o + \frac{b_i \, \eta_{\mathrm{rd},i} \, \eta_{\mathrm{sr}}(b_i)}{\eta_{\mathrm{sr}}(b_i) + \eta_{\mathrm{rd},i}} \right] \right\}^2 - b_i p_i,$$
$$\text{s.t.} \ \ b_i \geq 0. \quad (17)$$

The solution to the above optimization problem (17) gives the optimal spectrum demand denoted as $\mathscr{D}_i(p_i)$, which is given in the following proposition.

Proposition 1. *The optimal spectrum demand as a function of the unit price can be expressed as*

$$\mathscr{D}_i(p_i) = \begin{cases} b_i^{\mathrm{root}} & 0 < p_i < 2\omega\eta_{\mathrm{rd},i}\left(R_N - \overline{C}_o\right), \\ 0 & p_i \geq 2\omega\eta_{\mathrm{rd},i}\left(R_N - \overline{C}_o\right). \end{cases} \quad (18)$$

where b_i^{root} refers to the single positive root of the equation

$$\left[R_N - \overline{C}_o - C_{R,i}(b_i) \right] \mathcal{T}(b_i) = \frac{p_i}{2\omega}. \quad (19)$$

Proof. To solve the optimization problem (17), we should firstly check the convexity of the objective function. The second derivative of (16) with respect to b_i can be expressed as $\frac{\mathrm{d}^2\mathcal{U}_i}{\mathrm{d}b_i^2} =$

$$-2\omega\mathcal{T}^2(b_i) \quad (20)$$
$$-\frac{2\omega\eta_{\mathrm{rd},i}^2 r_i^2 \left\{ R_N - \left[\overline{C}_o + C_{R,i}(b_i) \right] \right\}}{\ln 2 \, b_i \left(\eta_{\mathrm{sr}}(b_i) + \eta_{\mathrm{rd},i} \right)^3 (b_i + r_i)^2} \left[\eta_{\mathrm{sr}}(b_i) + \eta_{\mathrm{rd},i} + \frac{2}{\ln 2} \right],$$

where $\mathcal{T}(b_i)$ denotes the first derivative of the $C_{R,i}(b_i)$ given in (14). Note that the nominal rate of the FSO link R_N is much larger than the hybrid link capacity in adverse weather conditions as mentioned before, i.e., $R_N \geq \overline{C}_o + C_{R,i}(b_i)$. From (20) one can see that for $b_i \geq 0$, $\frac{\mathrm{d}^2\mathcal{U}_i}{\mathrm{d}b_i^2} < 0$ always holds, therefore the objective function in (17) is concave. The optimal b_i can therefore be calculated through the KKT conditions. The Lagrangian associates with this optimization problem can be written as

$$\mathscr{L} = -\mathcal{U}_i - \gamma_1 b_i. \quad (21)$$

and the corresponding KKT conditions can be expressed as

$$b_i \geq 0, \ \gamma_1 \geq 0, \ \gamma_1 b_i = 0, \ \mathrm{d}\mathscr{L}/\mathrm{d}b_i = 0. \quad (22)$$

Firstly, let's consider the case when $b_i > 0$. Since the inequality $\gamma_1 \geq 0$ should hold, the equality $\gamma_1 b_i = 0$ necessitates $\gamma_1 = 0$. Substituting $\gamma_1 = 0$ into $\mathrm{d}\mathscr{L}/\mathrm{d}b_i = 0$, this equality can be expressed as

$$\frac{\mathrm{d}\mathscr{L}}{\mathrm{d}b_i} = -\frac{\mathrm{d}\mathcal{U}_i}{\mathrm{d}b_i} = -2\omega\left[R_N - \overline{C}_o - C_{R,i}(b_i) \right] \mathcal{T}(b_i) + p_i = 0. \quad (23)$$

After some algebraic manipulation, the equation above can be rewritten as

$$\left[R_N - \overline{C}_o - C_{R,i}(b_i) \right] \mathcal{T}(b_i) = \frac{p_i}{2\omega}. \quad (24)$$

Denoting the function with respect to b_i on the left hand side of (24) as $\mathcal{F}(b_i)$, i.e., $\mathcal{F}(b_i) = \left[R_N - \overline{C}_o - C_{R,i}(b_i) \right] \mathcal{T}(b_i)$. It can be proved that first order derivative of $\mathcal{F}(b_i) = \frac{1}{2\omega} \frac{\mathrm{d}^2\mathcal{U}_i}{\mathrm{d}b_i^2} < 0$. Therefore $\mathcal{F}(b_i)$ is a monotonically decreasing function for $b_i \geq 0$. When $b_i = 0$ we have $\mathcal{F}(0) = \eta_{\mathrm{rd},i}\left(R_N - \overline{C}_o \right)$ and with the increase of b_i, $\mathcal{F}(b_i) \to 0$. As a result, as long as $\eta_{\mathrm{rd},i}\left(R_N - \overline{C}_o \right) > p_i/2\omega$ holds, a single positive root of (24), denoting as b_i^{root}, always exists, which can be calculated numerically. This root is the desired optimal borrowed spectrum. On the other hand, when $b_i = 0$ holds, the equality $\mathrm{d}\mathscr{L}/\mathrm{d}b_i = 0$ can be rewritten as

$$\frac{\mathrm{d}\mathscr{L}}{\mathrm{d}b_i} = -2\omega\left[R_N - \overline{C}_o \right] \eta_{\mathrm{rd},i} + p_i - \gamma_1 = 0. \quad (25)$$

Since $\gamma_1 \geq 0$ should hold, the above equation requires that $\eta_{\mathrm{rd},i}\left(R_N - \overline{C}_o \right) \leq p_i/2\omega$.

Therefore the optimization problem (17) is solved completely as summarized in Proposition 1. ■

Corollary 1: It is interesting to investigate the behaviour of the spectrum demand $\mathscr{D}_i(p_i)$ with respect to the increase of the unit price p_i. Since $\mathcal{F}(b_i) = \left[R_N - \overline{C}_o - C_{R,i}(b_i) \right] \mathcal{T}(b_i)$ is a monotonically decreasing function, larger p_i results in smaller root of equation (19), i.e., b_i^{root}. Therefore, the demand function given in (18) is a monotonically decreasing function of the unit price in low p_i regime. This is a reasonable result

considering that with the increase of unit spectrum price, the source requires less spectrum demand due to the increase of the cost. However, with further increase of unit price, the cost of the RF spectrum becomes so high that borrowing the spectrum always results in the decrease of utility, the source quits the game and the demand spectrum becomes zero.

B. Utility of the Relays and the Supply Function

As mentioned in Section II, the RF nodes considered in this work have their own data to transmit to the destination. Although they can gain extra revenue by lending spectrum to the source, they may experience the QoS degradation of their connected UEs. Assuming that a RF node serves M_i UEs and each with a constant data rate requirement of R_i^{ur}, the utility of each RF node can be expressed as [20]

$$\mathcal{P}_i = b_i p_i + c_1 M_i - c_2 M_i \left(\left[R_i^{\mathrm{ur}} - \frac{(W_i - b_i)\,\eta_{\mathrm{rd},i}}{M_i} \right]^+ \right)^2, \tag{26}$$

where c_1 denotes the constant weight for the revenue of serving each local connection and c_2 denotes the constant weight for the cost of QoS degradation. The first term in (26) refers to the spectrum lending revenue based on linear pricing, the second term denotes the income of providing the service of local data transmission, and the third term is the cost due to the QoS degradation. In (26), it is assumed that the RF node charges a fixed fee for serving every connected UE to communicate with MBS so that its income of offering local service can be expressed as $c_1 M_i$. In addition, with the assumption that the remaining data rate is uniformly allocated to M_i UEs, the available data rate for each UE is $(W - b_i)\,\eta_{\mathrm{rd},i}/M_i$. Therefore, the cost induced by the QoS degradation of each UE can then be expressed as $c_2\big(\,[R_i^{\mathrm{ur}} - (W_i - b_i)\,\eta_{\mathrm{rd},i}/M_i]^+\,\big)^2$. This cost can be treated as the discount offered to the UE because of the spectrum lending to the source. The quadratic form of the QoS degradation cost has been widely used in literature [20], [30], [33], which indicates that the dissatisfaction of the UEs increases quadratically with the gap between the required data rate and the actual data rate. Note that this cost term also implies that when the required data rate is satisfied, the RF node would not offer any discounts to its UEs, as expected.

To establish a RF relay link $\mathcal{S} - \mathcal{R}_i - \mathcal{D}$, in our proposed spectrum trading game each RF node has to solve an optimization problem to get the optimal size of the leased spectrum for any given price p_i, which is the so-called spectrum supply function. This optimization problem is given by

$$\begin{aligned} &\max_{b_i}\ \mathcal{P}_i = b_i p_i + c_1 M_i - c_2 M_i \left(\left[R_i^{\mathrm{ur}} - \frac{(W_i - b_i)\,\eta_{\mathrm{rd},i}}{M_i} \right]^+ \right)^2, \\ &\text{s.t. } b_i \geq 0, \quad b_i \leq W_i. \end{aligned} \tag{27}$$

The first condition in (27) indicates that the leased spectrum is non-negative and the second inequality condition means that the leased spectrum should not exceed the total licensed spectrum of the RF node, i.e., W_i. The solution to the optimization problem (27) provides the optimal spectrum supply denoted as $\mathscr{S}_i(p_i)$, which is given in the following proposition.

Proposition 2. *The optimal spectrum supply as a function of the unit price can be expressed as*

$$\mathscr{S}_i(p_i) = \begin{cases} W_i - \frac{M_i R_i^{\mathrm{ur}}}{\eta_{\mathrm{rd},i}} + \frac{M_i p_i}{2c_2 \eta_{\mathrm{rd},i}^2}, & p_L < p_i < 2c_2 \eta_{\mathrm{rd},i} R_i^{\mathrm{ur}}, \\ W_i, & p_i \geq 2c_2 \eta_{\mathrm{rd},i} R_i^{\mathrm{ur}}, \\ 0, & \text{otherwise}, \end{cases} \tag{28}$$

where

$$p_L = \left(2c_2 \eta_{\mathrm{rd},i} \left[R_i^{\mathrm{ur}} - \frac{\eta_{\mathrm{rd},i} W_i}{M_i} \right] \right)^+. \tag{29}$$

Proof. To solve the optimization problem given in (27), we should firstly check the convexity of the objective function. By taking the second derivative of the objective function with respect to b_i, one can get $\mathrm{d}^2\mathcal{P}_i/\mathrm{d}b_i^2 = 0$ for $b_i \leq W_i - \frac{M_i R_i^{\mathrm{ur}}}{\eta_{\mathrm{rd},i}}$ and $\mathrm{d}^2\mathcal{P}_i/\mathrm{d}b_i^2 = -2c_2\eta_{\mathrm{rd},i}^2/M_i$ otherwise, which means that the objective function $\mathcal{P}_i$ is concave. Therefore, we can again use KKT conditions to get the optimal spectrum supply b_i. The Lagrangian function associated with the problem (27) is

$$\mathscr{L} = -\mathcal{P}_i - \gamma_2 b_i - \gamma_3 (W_i - b_i). \tag{30}$$

The corresponding KKT conditions for this optimization problem can be expressed as

$$\begin{aligned} &b_i \geq 0, \quad b_i \leq W_i, \quad \gamma_2, \gamma_3 \geq 0, \\ &\frac{\mathrm{d}\mathscr{L}}{\mathrm{d}b_i} = 0,\ \gamma_2 b_i = 0,\ \gamma_3 (W_i - b_i) = 0. \end{aligned} \tag{31}$$

Firstly, let's consider the case when $b_i > 0$. In this scenario, the equality $\gamma_2 b_i = 0$ necessitates $\gamma_2 = 0$. After some algebraic manipulations, the first derivative of $\mathscr{L}$ can be expressed as $\frac{\mathrm{d}\mathscr{L}}{\mathrm{d}b_i} =$

$$\begin{cases} -p_i + \gamma_3, & b_i \leq W_i - \frac{M_i R_i^{\mathrm{ur}}}{\eta_{\mathrm{rd},i}}, \\ -\Big[p_i - 2c_2 \eta_{\mathrm{rd},i} \Big(R_i^{\mathrm{ur}} - \frac{(W_i - b_i)\eta_{\mathrm{rd},i}}{M_i} \Big) \Big] + \gamma_3, & \text{otherwise}. \end{cases}$$

Assuming $b_i < W_i$, in order to make sure the equality $\gamma_3 (W_i - b_i) = 0$ in KKT conditions (31) is satisfied, the parameter γ_3 should be zero. Substituting $\gamma_3 = 0$ into $\mathrm{d}\mathscr{L}/\mathrm{d}b_i = 0$, one can get the optimal spectrum supply function denoted as $\mathscr{S}_i(p_i)$ given by

$$\mathscr{S}_i(p_i) = W_i - \frac{M_i R_i^{\mathrm{ur}}}{\eta_{\mathrm{rd},i}} + \frac{M_i p_i}{2c_2 \eta_{\mathrm{rd},i}^2}. \tag{32}$$

In order to ensure that the rest KKT conditions are all satisfied, this spectrum supply should also satisfy $0 < \mathscr{S}_i(p_i) < W_i$. By substituting (32) into this inequality and after some manipulations, we can get that a constraint on the given unit price p_i should be satisfied as $p_L < p_i < 2c_2 \eta_{\mathrm{rd},i} R_i^{\mathrm{ur}}$ where p_L is given in (29). However, outside this range of given price the KKT conditions cannot be all guaranteed and hence no optimal spectrum supply exists when $0 < b_i < W_i$. On the other hand, when $b_i = W_i$ holds, by substituting this into equality $\mathrm{d}\mathscr{L}/\mathrm{d}b_i = 0$, one can get $-(p_i - 2c_2\eta_{\mathrm{rd},i} R_i^{\mathrm{ur}}) + \gamma_3 = 0$. Considering that γ_3 is non-negative, this equality results in a constraint for the price as $p_i \geq 2c_2 \eta_{\mathrm{rd},i} R_i^{\mathrm{ur}}$. Therefore, as long as $p_i \geq 2c_2 \eta_{\mathrm{rd},i} R_i^{\mathrm{ur}}$ is met, we have the optimal spectrum supply $\mathscr{S}_i(p_i) = W_i$.

Secondly, when $b_i = 0$ holds, the inequality $\gamma_3 (W_i - b_i) =$

0 requires $\gamma_3 = 0$. Therefore, the Lagrangian function (30) can be rewritten as $\mathscr{L} = -\mathcal{P}_i - \gamma_2 b_i$. Considering the equality $\mathrm{d}\mathscr{L}/\mathrm{d}b_i = 0$ and inequality $\gamma_2 \geq 0$, it can be calculated that when the optimal leased spectrum is zero, the constraint $p_i \leq p_L$ should be satisfied.

The optimization problem (27) is solved completely as summarized in Proposition 2. ■

Corollary 2: The optimal spectrum supply given in (28) illustrates that with the increase of the unit price, the spectrum supply firstly fixes at zero and then increases with the increase of the unit price. Finally when the price is high enough, the relay is pleased to lend all of its licensed spectrum W_i to gain higher revenue.

C. Spectrum trading Process and Relay Selection

We have derived the demand function of the source given in (18) and the supply function of the relays given in (28). The remaining problem is how to reach the market-equilibrium price using these functions. The market-equilibrium is defined as the situation where the supply of an item is exactly equal to its demand [20], [28]. As discussed in Section III-A, the spectrum demand function is a decreasing function with respect to the price, which means higher price results in less spectrum demand due to the higher cost. One the other hand, as discussed in Section III-B, supply function is an increasing function with respect to the price, which in turn implies that higher price leads to more spectrum supply due to the higher revenue. Therefore, the cross point of these two functions (if exists), i.e.,

$$\mathscr{D}_i(p_i^*) = \mathscr{S}_i(p_i^*), \tag{33}$$

gives the market-equilibrium price p_i^* where the spectrum demand and supply are balanced. In this equilibrium, both source and RF node are happy with the price and size of the leased spectrum. Since an analytical expression of the root for (33) cannot be derived, we solve this equation numerically using bisection method. It is possible that the root of (33) corresponds to zero spectrum, i.e., $\mathscr{D}_i(p_i^*) = \mathscr{S}_i(p_i^*) = 0$. This indicates that no market-equilibrium price can be reached and the spectrum trading between the source and the RF node cannot be established. This could result from multiple practical conditions such as large number of UEs in RF node, large capacity requirement from the source, deep fading in dual-hop RF relay link and so on.

So far we mainly focused on the spectrum trading process between the source $\mathcal{S}$ and the ith RF relay $\mathcal{R}_i$. However, as illustrated in Fig. 1, there may be multiple surrounding RF node candidates that can act as the relay for the source. Therefore, a relay selection method needs to be developed. When $\overline{C}_o < C_{th}$ is satisfied due to the presence of adverse weather conditions, the source will notify the distributed N available RF nodes and broadcast some information including the current average FSO link capacity and the nominal rate of the FSO link in clear weather. Assuming that all RF nodes know the form of the source demand function given in (18), each RF node is able to generate the exact demand function of the source. In addition, based on its own traffic load information such as the number of connected UEs and their data rate requirements, every RF node can also generate its own supply function using the equation given in (28). With both calculated demand and supply functions, every RF node could calculate its proposed market-equilibrium unit spectrum price p_i^* using (33) as well as the corresponding optimal portion of leased spectrum to offer. The RF nodes then send this information back to the source. Having the proposed price and the optimal leased spectrum from each RF node, the source is able to calculate its own utility using (15) to finally select the RF node which provides it with the maximal utility. After notifying the selected RF node, the source can use the leased bandwidth to establish a RF dual-hop relay link to improve the throughput. Note that the proposed spectrum trading game and relay selection will be restarted after each time interval T_u. In those scenarios where the RF nodes do not have access to the information of the source, the source and RF nodes should learn the behaviour of each other from the history and a distributed price adjustment algorithm should be carefully designed [20], which is out of the scope of this work.

TABLE I
THE PARAMETER SETTING [16], [17], [22]

FSO Link		
Symbol	Definition	Value
d	Receiver aperture diameter	5 cm
ρ	Responsivity of FSO photodetector	0.5 V^{-1}
L_{SD}	Distance between the source and destination	1000 m
ϕ	Beam divergence angle	3.5 mrad
C_n^2	Refraction structure index	5×10^{-14} $\mathrm{m}^{-2/3}$
λ_o	Laser wavelength	1550 nm
σ_o^2	Noise variance at FSO receiver	10^{-14} A^2
P_o	Optical transmission power at the source	20 mW
R_N	Nominal Rate of FSO link	1 Gbps
W_o	Bandwidth of FSO link	1 GHz
ω	Constant weight for the utility of the source	5×10^{-4}
RF Link		
Symbol	Definition	Value
λ_R	RF wavelength	85.7 mm
G_{TX}, G_{RX}	Antenna Gain	(10,10) dBi
L_{ref}	Reference distance of the RF link	80 m
$L_{R,i}^{(1)}$	Distance between source and RF nodes	600 m
$L_{R,i}^{(2)}$	Distance between RF nodes and destination	600 m
$P_R^{\mathcal{S}}$, $P_R^{\mathcal{R}}$	RF transmitter power at the source and the RF nodes	0.2 W
N_0	Noise power spectral efficiency at RF receiver	-114 dBm/MHz
W	Licensed spectrum for the $\mathcal{R}_i - \mathcal{D}$ link	20 MHz
R_i^{ur}	Data rate requirement per user equipment	3 Mbps
δ	RF path-loss exponent	3.5
c_1, c_2	Constant weights for the utility of the RF nodes	$(1, 0.5)$

IV. NUMERICAL RESULT ANALYSIS

In this section, we present some simulation results for our proposed system in the application of wireless backhauling as plotted in Fig. 1. Unless otherwise stated, the values of the system parameters used for the numerical simulations are listed in the Table I [16], [17], [22]. Note that for simplicity it is assumed that each RF relay has the same amount of total licensed bandwidth $W_i = W, \forall i \in \{1, \ldots, N\}$ and the RF fading coefficient $h_{R,i}^{(t)}$ is modelled as Rayleigh distribution [1], [21]. In addition, the transmitted RF power at the source

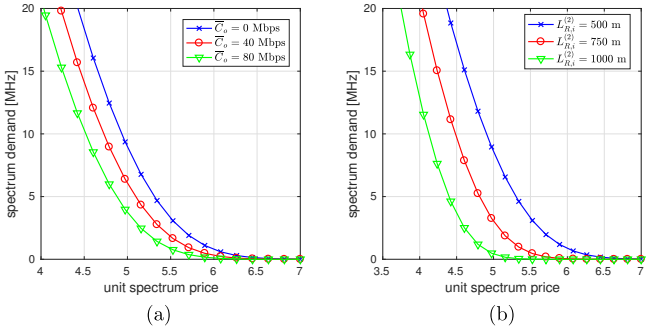

Fig. 3. The spectrum demand versus the unit spectrum price: (a) for different FSO link conditions; (b) for different distance between the RF node and destination with average FSO link capacity $\overline{C}_o = 40$ Mbps.

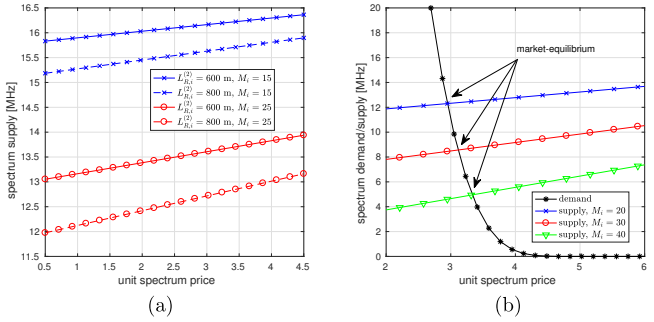

Fig. 4. (a) The spectrum supply versus the unit spectrum price for different numbers of connected UEs in the small cell and link distance between the relay and destination; (b) The demand and supply functions with respect to the unit spectrum price for different number of connected UEs in the small cell where $\overline{C}_o = 25$ Mbps and $h^{(1)}_{R,i} = h^{(2)}_{R,i} = 0.25$.

and the relays are considered to be equal, i.e., $P^{\mathcal{S}}_R = P^{\mathcal{R}}_R = P_R$ and the trigger capacity is $C_{th} = 80$ Mbps. The property of the market-equilibrium pricing in the absence of random RF channel fading is firstly presented and the communication performance improvement of employing the proposed spectrum trading strategy is then discussed.

A. Market-Equilibrium Pricing

Figure 3(a) plots the source demand function (18) with respect to the unit spectrum price p_i with various average FSO link capacities ($\overline{C}_o$). It is presented that the spectrum demand monotonically decreases with the increased of the spectrum price. For example, with $\overline{C}_o = 40$ Mbps when the unit spectrum price increases from 4.4 to 5.5, the spectrum demand reduces from 15.6 MHz to 1.6 MHz. One can also observe that those systems with worse FSO links are willing to buy more spectrum for a given price due to the higher cost introduced by the QoS degradation of the local service. For instance, with a given unit spectrum price 5 when $\overline{C}_o = 40$ Mbps, the spectrum demand is 6.38 MHz; however, when $\overline{C}_o = 80$ Mbps the corresponding spectrum demand drops to 3.96 MHz.

Besides the condition of FSO channel, the behaviour of the demand function is also associated with the locations of the RF nodes, which determines the data rate of the RF relay link. Figure 3(b) shows the effect of RF node locations to the demand function. The distance between the source and RF node is fixed at $L^{(1)}_{R,i} = 600$ m, whereas the the distance between the RF node and destination $L^{(2)}_{R,i}$ varies. The same results can also be observed when $L^{(1)}_{R,i}$ changes. This figure shows that, for a given unit spectrum price, lower $L^{(2)}_{R,i}$ results in higher spectrum demand. For example, the spectrum demand when $L^{(2)}_{R,i} = 500$ m is 8.97 MHz with a unit price 5; however, the corresponding bandwidth demand when $L^{(2)}_{R,i} = 750$ m is only 3.26 MHz. This is because smaller distance between the RF node and destination results in better channel condition in $\mathcal{R}_i - \mathcal{D}$ link. The source is then happy to buy more bandwidth, which can result in higher data rate to the destination and hence higher utility.

From the supply function given in (28), we know that the behaviour of the supply function is associated with both the location of the RF node and the number of connected UEs in RF node. Figure 4(a) plots the supply function versus the unit price with various number of connected UEs and distance between the RF node and destination. It is presented that with the increase of the unit price, the bandwidth supply increases. For instance, when $L^{(2)}_{R,i} = 600$ m and $M_i = 25$, the bandwidth supply is 13.1 MHz with a given spectrum price 1, whereas the corresponding bandwidth increases to 13.7 MHz when the spectrum price increases to 3.5. In addition, it is also obvious that with the increase of the distance $L^{(2)}_{R,i}$ and the number of connected local UEs M_i, the spectrum supply for a given price decreases due to the less total data rate to the destination and higher traffic load, respectively.

Figure 4(b) shows both supply and demand functions with respect to the unit spectrum price under different number of connected UEs in the small cell. The market-equilibrium price is given by the cross-point when the supply function meets the demand function. One can obverse that with the increase of the connected UE number in the RF node, the market-equilibrium price increases and the corresponding leased spectrum decreases as expected. For example, when $M_i = 20$ the market-equilibrium price is 2.95 and the leased spectrum is 12.3 MHz; however, the corresponding price increases to 3.3 and the leased spectrum decreases to 4.9 MHz when $M_i = 40$ due to the high traffic load for RF node. We would like to emphasize that beside the number of connected UEs, the the market-equilibrium is also associated with many other conditions, i.e., the FSO link condition, the distance between the source (RF node) and RF node (destination), and also the fading conditions of RF links.

B. Performance Improvement

Now let's consider the performance improvement achieved by the proposed system in the wireless backhauling application involving the randomness of the Rayleigh fading in RF links and the traffic load in RF nodes. We assume that the data rate requirement of each UE in the small cell R^{ur}_i is a constant; however, the traffic load of the SBS varies due to the random number of connected UEs M_i, which is modelled as a Poisson distributed random variable with mean υ_M.

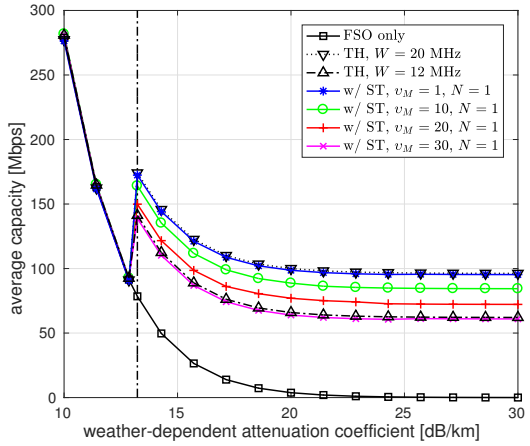

Fig. 5. The average capacity versus the weather-dependent attenuation coefficient of the FSO link κ with a single RF node involved in the spectrum trading, i.e., $N = 1$, and various average number of connected UEs υ_M in the small cell. The vertical dashed-dotted line represents the κ which results in an average capacity of FSO link equal to the threshold C_{th}. ST: spectrum trading; TH: traditional hybrid RF/FSO link.

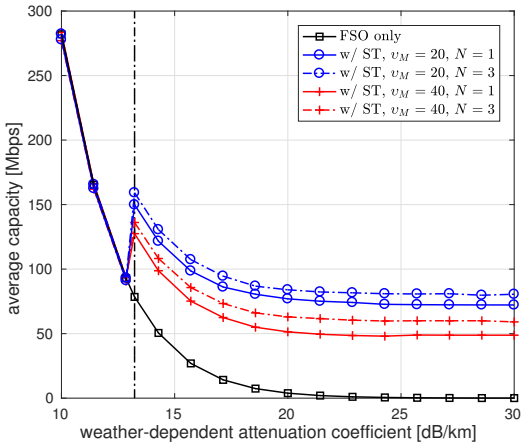

Fig. 6. The average capacity versus the weather-dependent attenuation coefficient of the FSO link κ with various υ_M under different number of surrounding small cells N. The vertical dashed-dotted line represents the κ which results in an average capacity of FSO link equal to the threshold C_{th}. ST: spectrum trading; TH: traditional hybrid RF/FSO link.

Figure 5 presents the average capacity versus weather-dependent attenuation coefficient κ with various υ_M with and without the spectrum trading. Note that in this figure a single RF node locating at $L^{(1)}_{RF,i} = L^{(2)}_{RF,i} = 600$ m is considered, i.e., $N = 1$, and in order to get accurate average capacity performance, 3×10^3 samples of channel realizations are generated for each κ. From Fig. 5 one can observe that with the increase of κ the average capacity for FSO-only link decreases significantly and when κ is above 20 dB/km the capacity of FSO link becomes negligible. However, in the presence of proposed spectrum trading, as long as the average FSO capacity is less than the trigger rate $C_{th} = 80$ Mbps (or equivalently when $\kappa > 13.23$ dB/km), the average capacity of the system can be significantly improved by means of establishing the dual-hop RF/FSO hybrid link. For instance, an average capacity of 144 Mbps can be achieved when $\kappa = 14.3$ dB/km and $\upsilon_M = 1$ when spectrum trading is employed; however, for FSO system without spectrum trading the corresponding average capacity is only 50 Mbps. In addition, it is also presented that the performance of systems with smaller υ_M outperforms those with larger υ_M as expected, because of the lower probability of high traffic loads in RF nodes. Furthermore, with the increase of attenuation coefficient κ, the average capacities of systems with spectrum trading decrease and finally saturate at fixed values. For example, the asymptotic average capacities at high κ are 84.4 and 60.9 for systems with $\upsilon_M = 10$ and $\upsilon_M = 30$, respectively. This is because when $\kappa \to \infty$, the FSO link is totally non-functional and the throughput from the source to the destination thoroughly relies on the dual-hop RF relay link, which provide the source with a fixed average capacity. The performance of a typical traditional hybrid RF/FSO link is also presented in this figure. To have a fair comparison with the proposed system in terms of link geometry, it is assumed that a dedicated dual-hop RF link is employed in the traditional link to support the FSO link when its capacity is below the same trigger rate C_{th}. One can observe that the average capacity of the proposed system with $\upsilon_M = 1$ is close to the traditional hybrid link with 20 MHz RF spectrum. Similarly, the average capacity of the system with $\upsilon_M = 30$ is close to that of the traditional link with 12 MHz RF spectrum.

Figure 6 plots the performance of the average capacity with various number of surrounding RF small cells N. It is shown that by increasing N better average capacity performance can be achieved. For instance, by increasing $N = 1$ to $N = 3$, the average capacity increases from 48 Mbps to 60 Mbps for $\upsilon_M = 40$ and $\kappa = 24$ dB/km. Accordingly, when $\upsilon_M = 20$ the average capacity rises from 72.7 Mbps to 80.9 Mbps. This is because when the FSO link is unavailable due to the adverse weather conditions, with larger N the source has more SBS candidates to choose and when one SBS is in high traffic load and/or in deep fading, the source is able to look for the other SBSs to buy the RF spectrum. Therefore the probability of establishing high throughput dual-hop RF relay link increases with the increase of N, which leads to better performance. In fact, the effect of relay selection in this work is similar to the selection combining in the context of spatial diversity where the most favourable signal at the receiver among several received signals is selected for decoding. The difference is that in this work, the RF node that the source selects is the one which provides the source with highest profit.

It is anticipated that with the increase of N, higher profit of the source should be achieved. To justify this point, the asymptotic profit of the source in high κ versus N is plotted in Fig. 7(a). It is presented that for a fixed number of surrounding RF nodes, the source can achieve higher profits when the RF nodes are with less traffic loads. In addition, for all systems with various traffic load conditions, significant utility improvement with the increase of surrounding RF nodes can be achieved. For example, when there is only one surrounding RF node, the average profit of the source is 4.43 when $\upsilon_M = 40$; however, the corresponding profit increases to 9.37

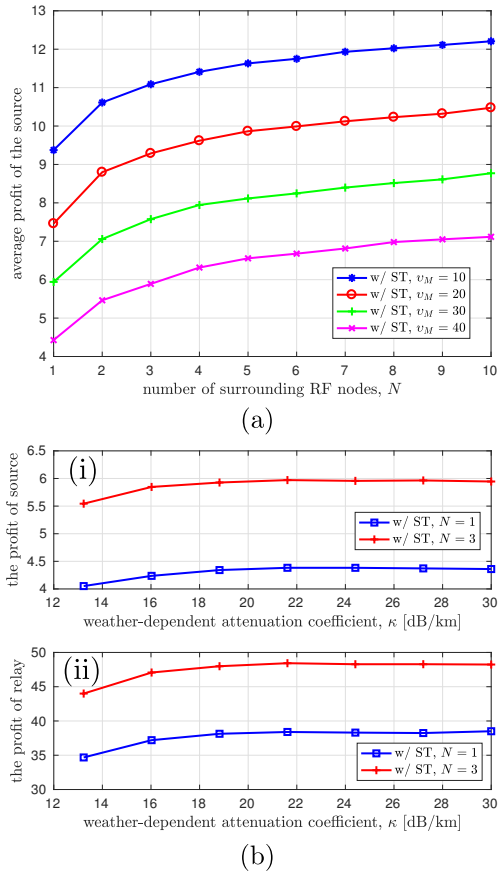

Fig. 7. (a) The asymptotic profit of the source versus the number of surrounding RF nodes N in high κ regime for various υ_M. (b) The gained profit versus the weather-dependent attenuation coefficient of the FSO link with $\upsilon_M = 40$ for various N: (i) the profit of the source gained from ST; (ii) the total profit of RF nodes gained from ST. ST: spectrum trading.

when $\upsilon_M = 10$. When the number of surrounding RF node rises to 7, both profits increases, i.e., 6.8 for $\upsilon_M = 40$ and 11.9 for $\upsilon_M = 10$.

Figure 7(b) plots the profit of the source and RF nodes versus the weather-dependent attenuation coefficient of the FSO link. Note that the profits plotted in this figure refer to the extra profits gained from the spectrum trading, i.e., the difference of the profits in the presence and absence of spectrum trading, rather than the actual profits. In the upper figure of Fig. 7(b) it is presented that with the increase of κ, the profit of the source increases. This indicates that the source benefits more from the spectrum trading when the weather condition becomes worse. In addition, when higher number of surrounding RF nodes are involved in the game, e.g., increasing N from 1 to 3, the source can achieve higher profit due to the relay selection, as expected. Similar behaviour of the profit can also be observed at the RF node side as shown in the lower figure of Fig. 7(b). Note that when multiple RF nodes are involved, the total profit of the RF nodes gained from spectrum trading is plotted. It can be observed that when the weather condition becomes worse, the source prefers to buy more spectrum from the RF nodes and hence the nodes can achieve higher profit.

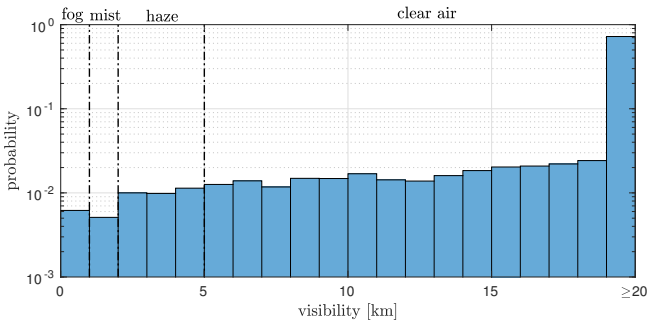

Fig. 8. The histogram of the hourly visibility for Edinburgh from January 2016 to June 2017.

Finally, let's consider the application of our proposed system in a realistic channel model based on the climate data for the city of Edinburgh. The measured hourly visibility data of the Edinburgh Gogarbank weather station for January 2016 to June 2017 (totally $\mathscr{H}_{\text{tot}} = 13128$ hours) is provided by the United Kingdom's national weather service the Meteorological Office. Fig. 8 shows the histogram of the hourly visibility. One can see that the probability of fog events (with visibility less than 1 km) which might severely degrade the FSO link performance is quite low (around 6×10^{-3}). This reveals that the hybrid RF/FSO links proposed in previous works [16] with RF links to be active continuously are not necessarily the most economical choice, since in most of the time FSO links perform well enough. The proposed system in this work benefits from establishing the hybrid link only when the low-frequent adverse weather conditions appear. Therefore, the proposed system would be only responsible for the cost of the RF spectrum for 0.6% of that in a traditional hybrid link with dedicated licensed RF link. In addition, compared to those hybrid links with licence-free RF spectrum, the expenditure of equipment, deployment and installation is significantly reduced.

In the simulation, we use the hours of fog events from the hourly visibility data (totally $\mathscr{H}_{\text{fog}} = 86$ hours) and assume that the coherence time of the weather conditions is $T_c = 1$ hour, the time-scale of the traffic load change in RF nodes T_t is 5 minutes, and the coherence time of the RF fading is $T_f = 3$ s. The weather-dependent coefficient κ can be calculated based on the visibility using (3). Figure 9 represents the simulation results and confirms that the FSO-only system is significantly outperformed by those systems with proposed spectrum trading between the source and RF nodes. It also shows that the system with relatively lower traffic loads in RF nodes ($\upsilon_M = 5$) performs the best. The average capacity of FSO-only system during these fog hours is only 52.5 Mbps; however, when the proposed system is employed and consider $\upsilon_M = 5$, the corresponding average capacity considerably increases to 129 Mbps.

It is also valuable to evaluate the link availability enhancement of the proposed system over FSO-only link. The availability is defined as the probability of time in which the atmospheric loss does not cause outage and it is usually calculated over a period of one or more years [34]. Considering

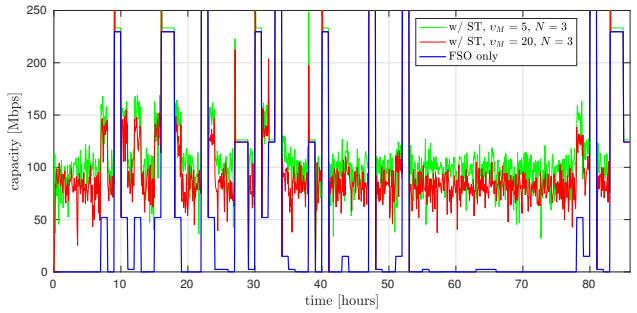

Fig. 9. The average capacity versus the hours with fog in Edinburgh from January 2016 to June 2017. ST: spectrum trading.

a specific data rate requirement, the availability of FSO-only link is given by $A_{\rm FSO} = (\mathscr{H}_{\rm tot} - \mathscr{H}_{\rm out})/\mathscr{H}_{\rm tot}$, where $\mathscr{H}_{\rm tot}$ denotes the total hours considered and $\mathscr{H}_{\rm out}$ is the number of outage hours when the required data rate is not achieved. On the other hand, when the proposed system is employed, the link availability can be expressed as

$$A_{\rm ST} = \frac{\sum_{j=1}^{\mathscr{H}_{\rm out}} \psi_j^{\rm ava} + (\mathscr{H}_{\rm tot} - \mathscr{H}_{\rm out}) \times 1}{\mathscr{H}_{\rm tot}}, \qquad (34)$$

where $\psi_j^{\rm ava}$ refers to the the availability probability of the proposed system at the jth outage hour experienced by the FSO-only system. Note that because of the randomness of the fading of RF link and traffic load in RF nodes, there might still remain a small probability of outage despite using the proposed system. Assuming that the minimum data rate requirement is 50 Mbps, one can calculate that the availability of FSO-only link is 99.5%. However, through Monte Carlo simulation it is demonstrated that by employing the proposed system and considering $\upsilon_M = 5$ and $N = 3$, the availability increases to 99.993%. Therefore, the proposed system enhances the availability of the FSO link by 2 nines. It is expected that the five-nine carrier-class availability can be achieved by involving the availability target into the design of the spectrum trading game and specifically into the optimization problem in (17).

V. Conclusion

In this work, a novel hybrid RF/FSO system based on the market-equilibrium spectrum trading is proposed. It is assumed that no RF spectrum is preallocated to the FSO link, but when the FSO link availability is significantly impaired by the infrequent adverse weather conditions, the source can borrow a portion of licensed RF spectrum from one of the surrounding RF nodes to establish a dual-hop RF/FSO hybrid link to maintain its throughput to the destination. Through numerical simulations, it is shown that in adverse weather conditions the proposed scheme can significantly improve the average capacity of the system especially when the surrounding RF nodes are with low traffic loads. In addition, with the increase of the number of RF nodes involved in the system, higher profit of the source can be achieved by means of diversity. The substantial enhancement of capacity and availability of the proposed system over FSO-only link is demonstrated by applying it into a realistic channel based on the Edinburgh weather statistics.

Acknowledgment

S. Huang and M. Safari gratefully acknowledge the financial support from EPSRC under grant EP/R023123/1 (ARROW).

References

[1] H. Dahrouj, A. Douik, F. Rayal, T. Y. Al-Naffouri, and M. S. Alouini, "Cost-effective hybrid RF/FSO backhaul solution for next generation wireless systems," *IEEE Wireless Commun.*, vol. 22, no. 5, pp. 98–104, Oct 2015.

[2] S. Huang and M. Safari, "Free-space optical communication impaired by angular fluctuations," *IEEE Trans. Wireless Commun.*, vol. 16, no. 11, pp. 7475–7487, Nov 2017.

[3] M. A. Khalighi and M. Uysal, "Survey on free space optical communication: A communication theory perspective," *IEEE Commun. Surveys Tutorials*, vol. 16, no. 4, pp. 2231–2258, Fourthquarter 2014.

[4] A. A. Farid and S. Hranilovic, "Outage capacity optimization for free-space optical links with pointing errors," *J. Lightw. Technol.*, vol. 25, no. 7, pp. 1702–1710, Jul 2007.

[5] S. Bloom, E. Korevaar, J. Schuster, and H. Willebrand, "Understanding the performance of free-space optics," *J. Opt. Netw.*, vol. 2, no. 6, pp. 178–200, Jun 2003.

[6] S. M. Navidpour, M. Uysal, and M. Kavehrad, "Ber performance of free-space optical transmission with spatial diversity," *IEEE Trans. Wireless Commun.*, vol. 6, no. 8, pp. 2813–2819, Aug 2007.

[7] M. Safari, M. M. Rad, and M. Uysal, "Multi-hop relaying over the atmospheric poisson channel: Outage analysis and optimization," *IEEE Trans. Commun.*, vol. 60, no. 3, pp. 817–829, Mar 2012.

[8] S. Arnon, J. Barry *et al.*, *Advanced optical wireless communication systems*. Cambridge university press, 2012.

[9] I. Kim, J. Koontz, H. Hakakha, P. Adhikari *et al.*, "Measurement of scintillation and link margin for the terralink laser communication system," in *Proc. SPIE*, vol. 3232, 1998, pp. 3232–3232–19.

[10] I. I. Kim and E. Korevaar, "Availability of free space optics (FSO) and hybrid fso/rf systems," in *Proc. SPIE*, vol. 4530, no. 84, 2001, pp. 84–95.

[11] M. Usman, H. C. Yang, and M. S. Alouini, "Practical switching-based hybrid FSO/RF transmission and its performance analysis," *IEEE Photonics Journal*, vol. 6, no. 5, pp. 1–13, Oct 2014.

[12] I. E. Lee, Z. Ghassemlooy, W. P. Ng, V. Gourdel, M. A. Khalighi *et al.*, "Practical implementation and performance study of a hard-switched hybrid FSO/RF link under controlled fog environment," in *2014 9th CSNDSP*, Jul 2014, pp. 368–373.

[13] Y. Tang, M. Brandt-Pearce, and S. G. Wilson, "Link adaptation for throughput optimization of parallel channels with application to hybrid FSO/RF systems," *IEEE Trans. Commun.*, vol. 60, no. 9, pp. 2723–2732, Sept 2012.

[14] S. Bloom and W. Hartley, "The last-mile solution: hybrid FSO radio," *Whitepaper, AirFiber Inc*, May 2002.

[15] T. Rakia, H. C. Yang, M. S. Alouini, and F. Gebali, "Outage analysis of practical FSO/RF hybrid system with adaptive combining," *IEEE Communications Letters*, vol. 19, no. 8, pp. 1366–1369, Aug 2015.

[16] W. Zhang, S. Hranilovic, and C. Shi, "Soft-switching hybrid FSO/RF links using short-length raptor codes: design and implementation," *IEEE J. Sel. Areas Commun.*, vol. 27, no. 9, pp. 1698–1708, Dec 2009.

[17] V. Jamali, D. S. Michalopoulos *et al.*, "Link allocation for multiuser systems with hybrid RF/FSO backhaul: Delay-limited and delay-tolerant designs," *IEEE Trans. Wireless Commun.*, vol. 15, no. 5, pp. 3281–3295, May 2016.

[18] M. Najafi, V. Jamali, and R. Schober, "Optimal relay selection for the parallel hybrid RF/FSO relay channel: Non-buffer-aided and buffer-aided designs," *IEEE Trans. Commun.*, vol. 65, no. 7, pp. 2794–2810, Jul 2017.

[19] X. Kang, R. Zhang, and M. Motani, "Price-based resource allocation for spectrum-sharing femtocell networks: A stackelberg game approach," *IEEE J. Sel. Areas Commun.*, vol. 30, no. 3, pp. 538–549, Apr 2012.

[20] D. Niyato and E. Hossain, "Market-equilibrium, competitive, and cooperative pricing for spectrum sharing in cognitive radio networks: Analysis and comparison," *IEEE Trans. Wireless Commun.*, vol. 7, no. 11, pp. 4273–4283, Nov 2008.

[21] U. Siddique, H. Tabassum, E. Hossain, and D. I. Kim, "Wireless backhauling of 5G small cells: challenges and solution approaches," *IEEE Wireless Commun.*, vol. 22, no. 5, pp. 22–31, Oct 2015.

[22] B. He and R. Schober, "Bit-interleaved coded modulation for hybrid RF/FSO systems," *IEEE Trans. Commun.*, vol. 57, no. 12, pp. 3753–3763, Dec 2009.

[23] A. Lapidoth, S. M. Moser, and M. A. Wigger, "On the capacity of free-space optical intensity channels," *IEEE Trans. Inf. Theory*, vol. 55, no. 10, pp. 4449–4461, Oct 2009.

[24] H. Izadpanah, T. ElBatt, V. Kukshya, F. Dolezal, and B. K. Ryu, "High-availability free space optical and RF hybrid wireless networks," *IEEE Wireless Commun.*, vol. 10, no. 2, pp. 45–53, Apr 2003.

[25] L. Ahumada, R. Feick, R. A. Valenzuela, and C. Morales, "Measurement and characterization of the temporal behavior of fixed wireless links," *IEEE Trans. Veh. Technol.*, vol. 54, no. 6, pp. 1913–1922, Nov 2005.

[26] P. Lin, J. Zhang, Q. Zhang, and M. Hamdi, "Enabling the femtocells: A cooperation framework for mobile and fixed-line operators," *IEEE Trans. Wireless Commun.*, vol. 12, no. 1, pp. 158–167, Jan 2013.

[27] Z. Zhang, J. Shi, H. H. Chen, M. Guizani, and P. Qiu, "A cooperation strategy based on nash bargaining solution in cooperative relay networks," *IEEE Trans. Veh. Technol.*, vol. 57, no. 4, pp. 2570–2577, Jul 2008.

[28] D. Niyato and E. Hossain, "Spectrum trading in cognitive radio networks: A market-equilibrium-based approach," *IEEE Wireless Commun.*, vol. 15, no. 6, pp. 71–80, Dec 2008.

[29] M. N. Tehrani and M. Uysal, "Pricing for open access femtocell networks using market equilibrium and non-cooperative game," in *2012 IEEE International Conference on Communications (ICC)*, Jun 2012, pp. 1827–1831.

[30] D. Niyato and E. Hossain, "Competitive pricing for spectrum sharing in cognitive radio networks: Dynamic game, inefficiency of nash equilibrium, and collusion," *IEEE J. Sel. Areas Commun.*, vol. 26, no. 1, pp. 192–202, Jan 2008.

[31] B. Wang, Z. Han, and K. J. R. Liu, "Distributed relay selection and power control for multiuser cooperative communication networks using stackelberg game," *IEEE Trans. on Mobile Computing*, vol. 8, no. 7, pp. 975–990, Jul 2009.

[32] M. J. Gans, N. Amitay, Y. S. Yeh *et al.*, "Outdoor BLAST measurement system at 2.44 GHz: calibration and initial results," *IEEE J. Sel. Areas Commun.*, vol. 20, no. 3, pp. 570–583, Apr 2002.

[33] P. Lin, J. Jia, Q. Zhang, and M. Hamdi, "Dynamic spectrum sharing with multiple primary and secondary users," *IEEE Trans. Veh. Technol.*, vol. 60, no. 4, pp. 1756–1765, May 2011.

[34] I. I. Kim, R. Stieger, J. Koontz *et al.*, "Wireless optical transmission of fast ethernet, FDDI, ATM, and ESCON protocol data using the terralink laser communication system," *Optical Engineering*, vol. 37, pp. 37–37–13, 1998.